This is a non-final version of an article published in final form in Exp Neurol. 2014 Mar;253:165-73. doi: 10.1016/j.expneurol.2013.12.020. Epub 2014 Jan 7.PMID: 24406455

Treatment with antibodies against TNF alpha protects against the neuropathy induced by the proteasoma inhibitor bortezomib in a mouse model

Albert Alé[1], Jordi Bruna[1], Marta Morell[1], Johan Monbaliu[2], Xavier Navarro[1], Esther Udina[1]

[1] Group of Neuroplasticity and Regeneration, Institute of Neurosciences and Department of Cell Biology, Physiology and Immunology, Universitat Autònoma de Barcelona, and Centro de Investigación Biomédica en Red sobre Enfermedades Neurodegenerativas (CIBERNED), Spain.

[2]Janssen Research and Development, Beerse Belgium

Corresponding author: Dr. Esther Udina, Faculty of Medicine, Universitat Autònoma de Barcelona, 08193 Bellaterra, Spain. Email: esther.udina@uab.cat

Acknowledgments

The authors thank the technical help of Monica Espejo and Jessica Jaramillo. We also acknowledge Janssen Research and Development, Johnson & Johnson Pharmaceutical companies and Millennium Pharmaceuticals, Inc., Cambridge, MA, USA , and for funding contribution and provision of bortezomib, and Janssen R&D, Radnor, PA USA for provision of anti-TNF-α and anti-IL-6 antibodies. This research was also supported by grant PI1100464 and TERCEL and CIBERNED funds from the Instituto de Salud Carlos III of Spain.

INTRODUCTION

Bortezomib (BTZ), a boronid acid dipeptide, is the first of a new class of chemotherapeutic drugs that inhibit the 20S proteasome complex. BTZ is an effective treatment for multiple myeloma (MM) and mantle cell lymphoma, and is under investigation in combination chemotherapy for treatment of other solid tumors (Richardson et al. 2003; Davies et al. 2009)

As the main dose limiting toxicity, BTZ induces a peripheral neuropathy, (Richardson et al. 2003; Badros et al. 2007; Mateos et al. 2008) purely sensory, length dependent, potentially painful and thus, suggestive of involvement of Aβ, Aδ and C primary afferent fibers. These symptoms prompt to reduce the dosage or even withdraw the treatment, consequently affecting the prognosis and the quality of life of the patients.

It is proposed that BTZ induces apoptosis of cancer cells by inhibiting NF-κB, leading to IL-6 and TNF-α reduction. This two proinflamatory cytokines are related with apoptosis and the adherent capabilities of cells (Chauhan et al., 1996; Wang 1998). However, the effects of BTZ on neurons are poorly known. In fact, both IL-6 and TNF-α increase after peripheral nerve insults like trauma injuries, or toxics. Interestingly, these cytokines are also increased in neuropathologies as Alzheimer disease, where the proteasome system is compromised. On the other hand, TNF-α increase is pointed as one of the key players in the development of neuropathic pain and small fiber pathology after neuronal insults. Therefore, in this study we want to analyse how BTZ is affecting the expression of these two cytokines in the neuronal tissue. These could be downregulate similarly to what it is observed in tumor cells or, in contrast, these could be urepgulated, following a neuroinflammatory pattern similar to the observed in other neural pathologies.

Therefore, we have evaluated how BTZ may affect the expression of TNF-α and IL-6, two of the most important cytokines implicated in neuroinflammation. We have used an animal model that has previously characterized in our lab, where the neuropathy induced by BTZ shows similar features to those described in patients. with a decrease in sensory nerve action potentials (SNAPs), partial loss of unmyelinated fibers in the skin, decrease in total number of myelinated axons, and reversibility after withdrawal (Bruna et al., 2010). As in humans, we observed selective involvement of sensory nerve conduction tests

without motor conduction abnormalities, suggesting that the toxicity was mostly affecting the sensory neurons located in the dorsal root ganglia (DRG).

Since both cytokines were markedly up-regulated on dorsal root ganglia after BTZ administration, we analyzed the effects of blocking these cytokines by administration of selective antibodies anti-TNF-α and anti-IL-6 on the evolution of the neuropathy. Anti-TNF-α but not IL-6 blockade was effectively reducing the neuropathic signs induced by BTZ administration.

MATERIAL AND METHODS

OF1 female mice aged 2.5 months were used in the study. The experimental procedures were approved by the ethics committee of the Universitat Autònoma de Barcelona, and were carried out in accordance with the European Community Council Directives.

mRNA analysis of cytokines

A batch of mice treated with BTZ at 1 mg/kg subcutaneously twice per week was used to analyze the mRNA expression of cytokines during the treatment. Four animals were sacrificed by decapitation after deep anesthesia before the treatment and at 2, 4 and 6 weeks after treatment. DRG, spinal cord and sciatic nerve were rapidly dissected, maintained in RNA-later solution (Qiagen, Barcelona, Spain) and processed for mRNA analyses. Total RNA was extracted using RNeasy Mini kit (Qiagen, Barcelona, Spain) including a DNase step (RNase free DNase set, Qiagen, Barcelona, Spain). One microgram of RNA was reverse-transcribed per sample using 10 µmol/L DTT, 200 U M-MuLV reverse transcriptase (New England BioLabs, Barcelona, Spain), 10 U RNase Out Ribonuclease Inhibitor (Invitrogen) and l µmol/L oligo(dT), 1 µmol/L of random hexamers (BioLabs, Beverly, MA, USA). The reverse transcription cycle conditions were 25ºC for 10 min, 42ºC for 1 h and 72ºC for 10 min. We analysed the mRNA expression of TNF-α, IL-6, TNF receptor 1 (TNFR1) and IL-6 receptor α (IL-6Rα). Glyceraldehyde 3-phosphate dehydrogenase (GAPDH) expression was used to normalize the expression levels of the different cytokines.

Gene-specific mRNA analyses were performed by SYBR-green real-time PCR using the MyiQ5 real-time PCR detection system (BioRad Laboratories, Barcelona, Spain). We previously fixed the optimal concentration of the cDNA to be used as template for each gene analysis to obtain reliable CT (threshold cycle) values for quantification. Realtime PCR amplification reactions contained the same amount of RT produc,t 10 µl of 2x QuantiMix EASY SYG KIT (Biotools, Madrid, Spain), 300 nM of forward and reverse primers and completed with nanopure water to obtain a final volume of 20 µl. The thermal cycling conditions comprised 3 min polymerase activation at 95ºC, 40 cycles of 10 s at 95ºC for denaturation and 30 s at 60ºC for annealing and extension, followed by a DNA melting curve for the determination of amplicon specificity. All experiments were performed in duplicate. CT values were obtained and analyzed with the BioRad Software. Fold change in gene expression was estimated using the CT comparative method ($2^{-\Delta\Delta T}$) normalizing to GAPDH CT values and relative to control samples. The fold-increase expression of samples during BTZ treatment with respect to basal samples was calculated for each transcript, and was based on real-time PCR threshold values. The mean value was obtained from three pools of the different nerve tissues per condition in each group.

DRG cultures

Coverslips placed in a 24 wells plate were *c*oated with 10µl/ml poly-D-lysine for two hours at 37º, washed, dried and further coated for two hours in 1µl/ml laminin. DRG were harvested from adult female mice treated with BTZ during 2 or 6 weeks and untreated mice as control. These were placed in Gey's salt solution (Sigma) with 6 mg/ml glucose. After peeling the DRG from connective tissue, samples were dissociated in 10% collagenase, 10% trypsin and 10% DNAse in Hanks without Ca-Mg for 30 min at 37ºC, with shaking every 10 minutes. Cells were resuspended in adult Neurobasal A medium (Gibco) supplemented with 1X B-27, 1X penicillin/strepetomycin, 1Mm L-glutamine and 6mg/ml glucose and plated on 24 wells plates for 24 hours.

Wells were fixed in 4% paraformaldehyde for 20 minutes, blocked with 1.5 % normal donkey antiserum (Millipore) and incubated 2 hours with antibodies anti β-tubulin-type III (1:1000, Covance), anti TNF-α (1:200, R&D Systems) or anti neurofilament heavy chain (1:1000, Millipore), followed by 1 hour in secondary antibody.

In vivo treatment with antibodies against IL-6 and TNF-α

BTZ treatment was given at 1 mg/kg subcutaneously twice per week for 6 weeks (on days 1-4-8-11-15-18-22-25-29-32-36-39) (Bruna et al., 2010). Mice were distributed in the following groups according to the administered treatments:

- Group BTZ (n=15) received only BTZ treatment and vehicle, and was designed as a reference group
- Group anti-IL-6 (n=13) received the same dosage of BTZ and 1 mg once per week of anti IL-6 intraperitoneally
- Group anti TNF-α (n=13) received the same dosage of BTZ and 0.1 mg twice per week of anti TNF-α intraperitoneally
- Group control (n=5) was constituted by untreated mice.

Functional evaluation

The functional state of the peripheral nerve was assessed by nerve conduction, rotarod and algesimetry tests. Functional evaluations were performed at baseline, before starting treatments, and then at 4 and 6 weeks of treatment.

For nerve conduction studies, the sciatic nerve was stimulated through a pair of needle electrodes percutaneously placed at the sciatic notch (proximal site) and at the ankle (distal site). Rectangular electrical pulses (Grass S88 stimulator) of 0.01 ms duration were applied up to 25% above the voltage that gave a maximal response. The compound muscle action potential (CMAP) was recorded from the plantar interosseus muscle with microneedle electrodes. Similarly, the sensory compound nerve action potential (SNAP) was recorded by electrodes placed at the fourth toe near the digital nerves (Navarro, et al., 1994; Verdú, et al., 1999; Bruna, et al., 2010). The onset latency and the maximal amplitude of the action potentials were measured and the nerve conduction velocity (NCV) of motor and sensory nerve fibers was calculated. During electrophysiological tests, the animals were under anesthesia (pentobarbital 40 mg/kg i.p.) and placed on a warm flat surface to maintain body temperature.

A rotarod apparatus for small rodents (LIAP) was used to assess general sensory-motor function. Mice were placed on the rod, turning at 8 rpm, and the time that each

animal remained on it before falling was measured. The value for a test was the mean of three trials separated by 10 minutes resting intervals. The ability to remain on the rotarod for 120 seconds was taken as an index of normality (Verdú, et al., 1999).

The plantar algesimetry technique was used to evaluate nociceptive C fibers function. Mice were placed into a plastic box with an elevated glass floor (Plantar Algesimeter, Ugo Basile) and the light of a projection lamp was focused onto the plantar surface of one hindpaw. The time to withdraw the heated paw was obtained from a time-meter coupled with infrared detectors. The value for a test was the mean of three trials separated by 10 min of resting periods.

Histological methods

At the end of the treatment animals were deeply anaesthetized and intracardialy perfused with paraformaldehyde (4% in PBS). A segment of the sciatic nerve at mid-thigh was removed. The samples were fixed in glutaraldehyde-paraformaldehyde (3%:3%), washed in cacodylate buffer, post-fixed with 2% osmium tetroxide, dehydrated in graded concentrations of ethanol and embedded in epon. Light microscopy observations were performed on 0.5 μm semithin sections stained with toluidine blue. Myelinated fiber counts were made from systematically selected fields at 1000x final magnification using Image J software (NIH, Bethesda MA). The density of myelinated nerve fibers was then derived (Gómez, et al., 1996; Bruna et al., 2010).

Plantar pads removed from perfused mice after the end of treatments were postfixed in Zamboni's fixative overnight and thereafter cryoprotected. Cryotome sections 70 μm thick were washed free-floating in PBS with 0.3% Triton-X100 and 1% normal goat serum for 1 h, then incubated in primary rabbit antiserum against protein gene product 9.5 (PGP, 1:1000; Ultraclone). After washes, sections were incubated in secondary antiserum conjugated to cyanine 3 (Navarro, et al., 1995). The sections were mounted on gelatin coated slides and viewed in an epifluorescence microscope (Olympus BX51) using appropriate filters. Five sections from each sample were used to quantify the number and density of epidermal nerve fibers present in the epidermis of the paw pads.

DRG removed from other mice after 1 and 2 weeks of treatment were fixed in 4% paraformaldehid and thereafter cryopotected. Cryotome sections 10 μm thick were washed

free-floating in PBS with 0.3% Triton-X100 and 1% normal goat serum for 1 h, then incubated in primary rabbit antiserum against β-tubulin-type III (1:1000, Covance) anti TNF-α (1:200, R&D Systems). After washes, sections were incubated in secondary antiserum conjugated to cyanine 3, and viewed under epifluorescence microscopy.

Data analysis

Results are expressed as mean and standard error. The results of functional tests during the study period are expressed as the percentage with respect to baseline values for each mouse. Comparisons between experimental groups in functional tests were made using repeated measures ANOVA, whereas one-way ANOVA was used to asses differences between groups in histological and immunohistochemical results. Statistical comparisons for real-time PCR results were made by one-way ANOVA. Bonferroni test was used as the post hoc test when needed. A p value less than 0.05 was considered as significant.

RESULTS

mRNA expression of proinflammatory cytokines during BTZ treatment

We found a high increase in mRNA expression of both TNF-α and IL-6 in DRG during the 6 weeks of BTZ treatment. Just 1 week after treatment DRG showed the higher expression levels of TNF-α (15.5 ±1.45). This increase was followed at the second week with a higher peak of IL-6 expression (22.02 ± 6.64) (Fig 1C). At later time points, levels decreased but were still higher than control ones and, thus, suggestive of a chronic overexpresion (4.43 ±1.31 of TNF-α and 4.62 ± 0.79 of IL-6 at the end of the treatment). Interestingly, in sciatic nerve and spinal cord mRNA levels of both cytokines were not affected or only slightly increased (Fig 1A and B). Levels of mRNA of the cytokine receptors TNFR-1 and IL-6Rα followed the same pattern of changes observed for the cytokines in the analyzed tissues, but peak of expression of the receptor TNFR1 was one week later than peak of TNF-α expression (Fig. 1D).

To localize witch cells were over-expressing these cytokines, we performed an immunohistochemistry of DRG at different time points. At one week, high immunoreactivity against TNF-α was observed in neurons, more marked in some small

ones (Fig 2). Satellite cells, labeled against GFAP did not show an increased expression of TNF-α when compared to controls. TNF-α immunoreactivity in neurons was slightly decreased at two weeks (data not shows).

When DRG from animals treated with BTZ for 4 or 6weeks were harvested and dissociated, we observed that *neurons from these ganglia extended longer neurites than neurons from non treated ones (Fig. 3B-C). However, neurites from BTZ-treated animals presented abnormal varicosities. Immunocitochemistry against TNF-α showed that this cytokine was mainly expressed in the neuronal soma (Fig. 3A). Increased immunoreactivity for TNF-α was also observed in the swellings of neurites from treated* animals.

Effects of anti-TNF-α and anti-IL-6 treatment on the BTZ induced neuropathy

Nerve conduction test results

The CMAP amplitude of the plantar muscle was similar in all the groups during the follow-up (Fig. 4B). In contrast, the SNAP amplitude in animals treated with BTZ decreased from 2 weeks, with a reduction with respect to basal values of 40% at 4 weeks and 50% at 6 weeks. Treatment with anti-IL-6 did not significantly prevent the SNAP decrease, around 40% at 6 weeks. In contrast, treatment with anti-TNF-α partially prevented the reduction of the SNAP amplitude, which was declined a 25% at the end of the treatment. Values of group anti-TNF-α were significantly higher at 4 and 6 weeks compared to group BTZ (Fig. 4A).

Sensory-motor function

At basal conditions, all animals were able to maintain themselves on the rod around 120 s (112±14), whereas at 6 weeks, BTZ-treated and BTZ plus anti-IL-6 groups showed a significant decline in the time of sustained walking in the rod, with values of 87±25 for group BTZ group and 85±35 for group anti-IL-6. In contrast, animals treated with BTZ plus anti-TNF-α were able to maintain the position on the rod similar to the control group (104±20) (Fig. 5A).

Pain sensibility

Thermal algesimetry tests showed a progressive increase of withdrawal thresholds in BTZ treated mice. Basal values averaged 10.4±0.3 s, similar to those recorded in the control group during follow-up. At 6 weeks after treatment the withdrawal latency increased in group BTZ (12.69±0.66 s), whereas groups anti-IL-6 and anti-TNF-α maintained normal latencies (10.83±1.17 s and 9.83±0.97 s, respectively) (Fig. 5B).

Histopathological results

The sciatic nerves of all the BTZ-treated mice showed a well preserved architecture. Some signs of Wallerian degeneration were observed, but without marked infiltration of macrophages. In group BTZ there was a lower density of myelinated fibers in some regions of the transverse sections compared to control nerves (Fig. 6). The mean number of myelinated fibers of the sciatic nerve was significantly reduced in group BTZ with respect to control nerves, whereas in groups anti-TNF-α and anti-IL-6 there was only a slight decrease. The estimated number of myelinated fibers was significantly higher in the group treated with anti-TNF-α compared with the group that received BTZ alone (Table 1).

Skin innervation

The number of free nerve endings in the epidermis of plantar pads, labeled for PGP9.5, was significantly lower in BTZ and anti IL-6 groups than in anti-TNF-α and control groups ($p=0.005$). In contrast, group anti-TNF-α did not show differences in number of epidermal nerve fibers with respect to control group (Fig 7).

mRNA expression of proiflammatory cytokines after cotreatments

At the end of the treatment, all DRG were removed to analyze mRNA levels of TNF-α and IL-6. Anti-TNF-α treatment did not modify the increased expression of TNF induced by BTZ, but reduced levels of IL-6 and TNFR1 (68.4% and 67.4% respectively), whereas Anti-IL-6 treatment did not significantly modify the expression levels of both cytokines and TNFR1.

DISCUSSION

The results of this study show that TNF-α and IL-6 are over expressed during BTZ treatment, and that co-administration of antibodies anti-TNF-α, but not anti-IL-6, exerts a protective effect against BTZ induced peripheral neuropathy in an animal model.

To investigate the role of these pro-inflammatory cytokines in BTZ neurotoxicity, we used an animal model previously characterized in our laboratory (Bruna et al., 2010, 2011). In this model, BTZ induces a pure sensory neuropathy, without motor affectation. This selectivity is related to the vulnerability of peripheral nerve and DRG to toxics, due to the higher permeability of the peripheral *vasa nervorum* compared with the one of the blood brain barrier that isolates the central nervous system. In fact, when analysing how BTZ was affecting the expression of TNF and IL-6, we observed a marked increase in DRG but not in the spinal cord, where the blood brain barrier protects against the arrival of the toxic. Levels on the sciatic nerve were marginally increased, suggesting that BTZ exerts its main toxic effect in the DRG, and that Schwann cells are less responsive to proteasome inhibitor BTZ than sensory neurons (Fig 1A and B). Similary, Bennet group, that proposes that mitotoxicity plays a central role in BTZ neuropathy, has already shown that mitochondria of Schwann cells is less receptive to chemotherapy toxicity than neuronal one (Xiao, W. H. et al. 2011; Zheng, H. et al. 2012); thus, reinforcing the hypothesis that BTZ is primarily affecting primary sensory neurons.

When focusing on the DRG, we observed an early peak of TNF-α overexpression just after two doses of BTZ (one week of treatment), whereas overexpession of IL-6 was later on time (peak at two weeks)(Fig 1C and 2).

This increase of both cytokines in DRG is, somehow, surprising. The most supported theory about the antitumoral activity of BTZ is by inhibiting NF-κB, an inhibition that reduces the levels of IL-6 and TNF-α in different tumoral cells (Chauhan et al., 1996; Wang, 1998), and decreases TNFRs in multiple myeloma cells (Wang, 1998). In contrast, we observed a significant increase of both cytokines in primary sensory neurons. Since TNF-α and IL-6 are classically related with NF-κB, our findings suggest that NF-κB could be activated in BTZ induced neuropathy, although further studies have to be performed to confirm this hypothesis.

To localize the cells that are expressing TNF-α, we performed immunohistochemistry of slices and also of dissociated primary cultures from DRG of

treated animals. In both DRG slices and dissociated cultures, we found that the increased expression of TNF-A induced by BTZ was mainly located on neuronal somas, and not in satellite cells (Fig 2 and 3A). In agreement with our findings, expression and secretion of TNF-α from neurons has also been described after peripheral nerve and spinal cord injuries, stroke or neuropathologies as Alzehimer diseases (AD). In AD there is an important impairment of the proteasome system, and, in fact, a recent study describes an early increase of TNF-α in animal models of this disease, especially in neurons, and suggests that chronic neuronal TNF-α expression could promote inflammation and lead to neuronal cell death (Michelle C. Janelsins et al., 2008) Therefore, the early up-regulation of TNF-α on primary sensory neurons in the DRG of BTZ treated animals could trigger the neurotoxicity and lead to sensory impairment. To further corroborate the role of TNF-α in the neuropathy induced by BTZ we analysed the effect of anti-TNF-α and anti-IL-6 in the evolution of the neuropathy.

We observed that anti-TNF-α treatment but not anti-IL6 treatment neuroprotected against BTZ neurotoxicity, thus suggesting that TNF-α is playing a major role, in this neuropathy. The neuroprotective effects of anti-TNF-α administration sustains the finding of a previous work reporting that 6 of 9 patients with neuropathy induced by BTZ had a significant improvement in their symptoms after treatment with lenalidomide, an antitumoral drug that downregulates TNF-α (Badros et al., 2007).

Anti-TNF-α treatment partially reverted the loss of SNAP amplitude (Fig. 4a), and myelinated fibers in the sciatic nerve, whereas completely preserved epidermal nerve fibers in the skin of mice (Table 1). Since epidermal nerve fibers are the smaller ones, these fibers could be more dependent on the TNF-α pathway than myelinated ones. In fact, when analysing by immunohistochemistry DRG of BTZ treated animals, small diameter neurons, compatible with the nociceptive ones, showed the higher expression of TNF-α when compared to bigger neurons. Therefore, TNF-α would affect more the smaller neurons and thus, explain the stronger effects of anti-TNF-α in small diameter fibers than in the bigger ones.

Anti-TNF-α treatment did not affect TNF-α upregulation induced by BTZ but reverses the increased expression of TNFR1, thus suggesting that this receptor is mediating

the toxic effect of TNF-α. Moreover, TNF-α is also decreasing IL-6 levels. TNF-α is an early event that triggers the proinflammatory response (Lee, et al., 2009). Therefore, blockade of TNF-α not just blocks the TNF-α pathway but also the expression of other pro-inflammatory cytokines, among these IL-6. Therefore, the decreased levels of IL-6 by anti-TNF-α treatment are also indicative of an efficient blockade of this pathway. In contrast, anti-IL-6 treatment, that did not show a relevant neuroprotective effect, neither decrease TNFR1 or IL-6 expression.

Although IL-6 does not seem to play a key role in the induction of BTZ neuropathy, probably can explain the higher capability of dissociated neurons, harvested from animals treated with BTZ, to extend longer neurites in cultures. Besides the neurotoxicity of BTZ, cultures of DRG from treated animals showed an increased capacity to extend neurites at 24 h, when control neurons hardly extend any (Fig. 3B and C). Since neurons were *in vivo* treated with BTZ prior to their culture, it seems that BTZ could mimic the conditioning lesion effect. In the conditioning lesion paradigm, an injury to the peripheral nerve prior to harvesting DRG, strongly potentiates the elongation of sensory neurites when later cultured *in vitro* (Smith and Skene, 1997). Since IL-6 is a key player in the conditioning lesion effect (Cafferty et al., 2004; Cao et al., 2006). BTZ might "condition" the primary sensory neurons by increasing their expression of proinflammatory cytokines. Since BTZ is mainly changing the expression of pro-inflammatory cytokines in neuronal somas and not satellite cells or nerve Schwann cells, ,it seems that inhibition of proteasome may directly alter the gene expression of the affected neurons, mimicking signals triggered by axotomy. On the other hand, this increased ability of treated neurons to elongate neurites could explain the marked recovery observed after withdrawal of BTZ treatment (Bruna et al 2011) by facilitating regeneration of the loss axons due to the toxic insult.

In conclusion, our findings indicates that blockade of TNF-α protects against the neuropathy induced by BTZ, preserving the functional decline of the SNAP amplitude, reducing the decrease of myelinated axons in the sciatic nerve and completely preventing small fiber loss in the skin. On the other hand, although BTZ induces also an increase of IL-6 levels, blocking this cytokine caused limited beneficial effects on BTZ induced neuropathy. Therefore, co-administration of anti-TNF-α in BTZ therapy may be a promising strategy to prevent the development of neuropathic complications. On the other

hand, studies to investigate the role of TNF-α pathway and how BTZ could differentially upregulate NF-κB in tumoral and neuronal cells are needed to further dilucidate the ethiopathogenesis of this neuropathy.

REFERENCES

Badros, A., Goloubeva, O., Dalal, J. S., Can, I., Thompson, J., Rapoport, A. P., Heyman, M., et al. (2007). Neurotoxicity of bortezomib therapy in multiple myeloma: a single-center experience and review of the literature. *Cancer* 110, 1042–9.

Bruna, J., Alé, A., Velasco, R., Jaramillo, J., Navarro, X., Udina, E. (2011). Evaluation of pre-existing neuropathy and bortezomib retreatment as risk factors to develop severe neuropathy in a mouse model. *J Periph Nerv Syst*, 16, 199–212.

Bruna, J., Udina, E., Alé, A., Vilches, J. J., Vynckier, A., Monbaliu, J., Silverman, L., et al. (2010). Neurophysiological, histological and immunohistochemical characterization of bortezomib-induced neuropathy in mice. *Expl Neurol*, 223, 599–608.

Cafferty, W. B. J., Gardiner, N. J., Das, P., Qiu, J., McMahon, S. B., Thompson, S. W. N. (2004). Conditioning injury-induced spinal axon regeneration fails in interleukin-6 knock-out mice. *J Neurosci*, 24, 4432–4443.

Cao, Z., Gao, Y., Bryson, J. B., Hou, J., Chaudhry, N., Siddiq, M., Martinez, J., et al. (2006). The cytokine interleukin-6 is sufficient but not necessary to mimic the peripheral conditioning lesion effect on axonal growth. *J Neurosci*, 26, 5565–5573.

Chauhan, B. D., Uchiyama, H., Akbarali, Y., Urashima, M., Yamamoto, K., Libermann, T. A., Anderson, K. C. (1996). Multiple myeloma cell adhesion-induced interleukin-6 expression in bone marrow stromal cells involves activation of NF-κB. *Blood*, 87, 1104–1112.

Davies AM, Chansky K, Lara PN Jr, Gumerlock PH, Crowley J, Albain KS, Vogel SJ, Gandara DR, Southwest Oncology Group (2009). Bortezomib plus gemcitabine/carboplatin as first-line treatment of advanced non-small cell lung cancer: a phase II Southwest Oncology Group Study (S0339). J Thorac Oncol 4:87–92.

Filosto, M., Rossi, G., Pelizzari, A. M., Buzio, S., Tentorio, M., Broglio, L., Mancuso, M., et al. (2007). A high-dose bortezomib neuropathy with sensory ataxia and myelin involvement. *J Neurol Sci*, 263, 40–43.

Gómez, N., Cuadras, J., Batí, M., Navarro, X., (1996). Histologic assessment of sciatic nerve regeneration following resection and graft or tube repair in the mouse. *Restor. Neurol. Neurosci*. 10, 187–196

Janelsins, M. C., Mastrangelo, M. a, Park, K. M., Sudol, K. L., Narrow, W. C., Oddo, S., LaFerla, F. M., et al. (2008). Chronic neuron-specific tumor necrosis factor-alpha expression enhances the local inflammatory environment ultimately leading to neuronal death in 3xTg-AD mice. *The American journal of pathology*, *173*(6), 1768–82.

Lee, K.-M., Jeon, S.-M., Cho, H.-J. (2009). Tumor necrosis factor receptor 1 induces interleukin-6 upregulation through NF-kappaB in a rat neuropathic pain model. *Eur J Pain*, 13, 794–806.

Li, C., Chen, S., Yue, P., Deng, X., Lonial, S., Khuri, F. R., Sun, S.-Y. (2010). Proteasome inhibitor PS-341 (bortezomib) induces calpain-dependent IkappaB(alpha) degradation. *J Biol Chem*, 285, 16096–16104.

Mateos, M.V., Hernandez, J.M., Hernandez,M.T., Gutierrez, N.C., Palomera, L., Fuertes,M., Garcia-Sanchez, P., et al. (2008). Bortezomib plus melphalan and prednisone in elderly untreated patients with multiple myeloma: updated time-to-events results and prognostic factors for time to progression. *Haematologica*, 93*,* 560–565.

Myers, R. R., Campana, W. M., Shubayev, V. I. (2006). The role of neuroinflammation in neuropathic pain: mechanisms and therapeutic targets, *Neuroscience, 11*(1).

Navarro, X., Verdu, E., Buti, M., (1994). Comparison of regenerative and reinnervating capabilities of different functional types of nerve fibers. *Exp. Neurol*. 129, 217–224.

Navarro, X., Verdú, E., Wendelschafer-Crabb, G.,& Kennedy, W.R., (1995). Innervation of cutaneous structures in the mouse hindpaw: a confocal microscopy immunocy-tochemical study. *J. Neurosci. Res*. 41, 111–120.

Richardson, P.G., Barlogie, B., Berenson, J., Singhal, S., Jagannath, S., Irwin, D., Rajkumar, S.V., et al. (2003). A phase 2 study of bortezomib in relapsed, refractory myeloma. *N. Engl. J. Med*. 348, 2609–2617.

Smith, D. S., Skene, J. H. (1997). A transcription-dependent switch controls competence of adult neurons for distinct modes of axon growth. *J Neurosci*, 17, 646–58.

Verdu, E., Vilches, J.J., Rodriguez, F.J., Ceballos, D., Valero, A., Navarro, X., (1999). Physiological and immunohistochemical characterization of cisplatin-induced neuropathy in mice. *Muscle Nerve* 22*,* 329–340.

Wang, C. (1998). NF-κB antiapoptosis: Induction of TRAF1 and TRAF2 and c-IAP1 and c-IAP2 to suppress caspase-8 activation. *Science*, 28, 1680–1683.

Xiao, W. H., Zheng, H., Zheng, F. Y., Nuydens, R., Meert, T. F., Bennett, G. J. (2011). Mitochondrial abnormality in sensory, but not motor, axons in paclitaxel-evoked painful peripheral neuropathy in the rat. *Neuroscience*, 199, 461–469.

Zheng, H., Xiao, W. H., & Bennett, G. J. (2012). Mitotoxicity and bortezomib-induced chronic painful peripheral neuropathy. *Experimental neurology*, *238*(2), 225–234.

Figure legends

Figure 1: Expression of TNF-α, IL-6 and their receptors on different nerve tissue during Bortezomib treatment. Levels of both cytokines were sustainably high until the end of treatment on DRG , whereas they were just slightly increased in sciatic nerve at 2 weeks and on spinal cord at the end. Only a significant increase of IL-6 at the 6 weeks was observed on spinal cord (A and B). Expression peak of TNF-α in DRG preceded IL-6 and TNFR1 peak (C and D). Values expressed as mean and SEM.

* P<0.05,**P<0.01,***P<0.001, vs basal group.

Figure 2: Sections of DRGs immunolabeled against β-III-tubulin (green), DAPI (blue) and TNF-α (red), from a control (up) and an animals treated with BTZ for 1week (down). TNF-a collabels with β-III-tubulin, indicating that BTZ increases TNF-α expression on neurons specially on small ones (white arrows).20x magnification Scale bar; 50 μm

Figure 3: Fig. 3. Dissociated primary neurons from dorsal root ganglia of BTZ treated animals for 2 weeks, double-staining against B-III-tubuline (in green) and TNF-α (in red, A). TNF-a was mainly localized on neuronal cell body and was also present in neurites that suffered swelling, indicating pathological distribution of this cytokine along the neurite (A). Dissociated DRG neurons from control animals (B) and BTZ treated animals for two weeks (C), labeled with B-III-tubuline. Neurons from treated animals showed increased neurite elongation at 24h in culture compared to control ones. 50x magnifications A and 10x magnification in B -C

Figure 4: Mean amplitude of the digital nerve SNAP (A) and the plantar muscle CMAP(B), stimulating at the sciatic notch. Values are expressed as percentages with respect to baseline. Both anti-TNF-α and IL-6 treatments partially maintains the decrease of the SNAPs , but only significantly on anti-TNF-α group. CMAP were not altered by any treatment. Error bars SEM. * P<0.05,**P<0.01.

Figure 5: Rotarod test results, expressed as time of maintenance in the rotating rod relative to baseline (A). Algesimetry test results expressed as time to withdrawal to hot pain stimulation. (B). All the groups were treated during 6 weeks. Anti-TNF-α treatment preserved the sensory-motor function and reverts the hypoalgesia, in contrast to BTZ and BTZ+anti IL-6 groups . Values are expressed as percentage with respect to baseline. Error bars SEM. * $P<0.05$ ** $P<0.01$

Figure 6: Semithin sections of sciatic nerve at midthigh, in control animals (A), after 6 weeks of treatment with BTZ (D) or in co-treatment with anti TNF-α (B) or anti IL-6 (C). Decreased density of myelinated fibers by BTZ was prevented with anti TNF treatment.100x magnification. Scale bar; 20 μm

Table 1: Estimated counts of myelinated nerve fibers of the sciatic nerve at midthigh and of unmyelinated intraepidermical fibers at the skin paw. Values expressed as mean and SEM. *$P<0.05$ vs BTZ group

Figure 7: Sections of skin pads immunolabeled against PGP 9.5. Images from a representative hind paws of a control (A), anti TNF-α (B) anti IL-6 (C) and BTZ (D) animals. Estimated counting of ummyelinated fibers (D). Number of intraepidermical profiles was significantly higher in anti TNF-α respect to BTZ treatment. 20x magnification. Scale bar; 100 μm

Figure 8: Expression of TNF-α, IL-6 and their receptors on DRG at the end of the cotreatments. Anti -TNF-α cotreatment not affect up regulation of TNF-α but downregulate levels of TNFR1 and IL-6 expression , whereas no significant changes were observed IL-6 treatment. Values expressed as mean and SEM. *$P<0.05$ vs BTZ group

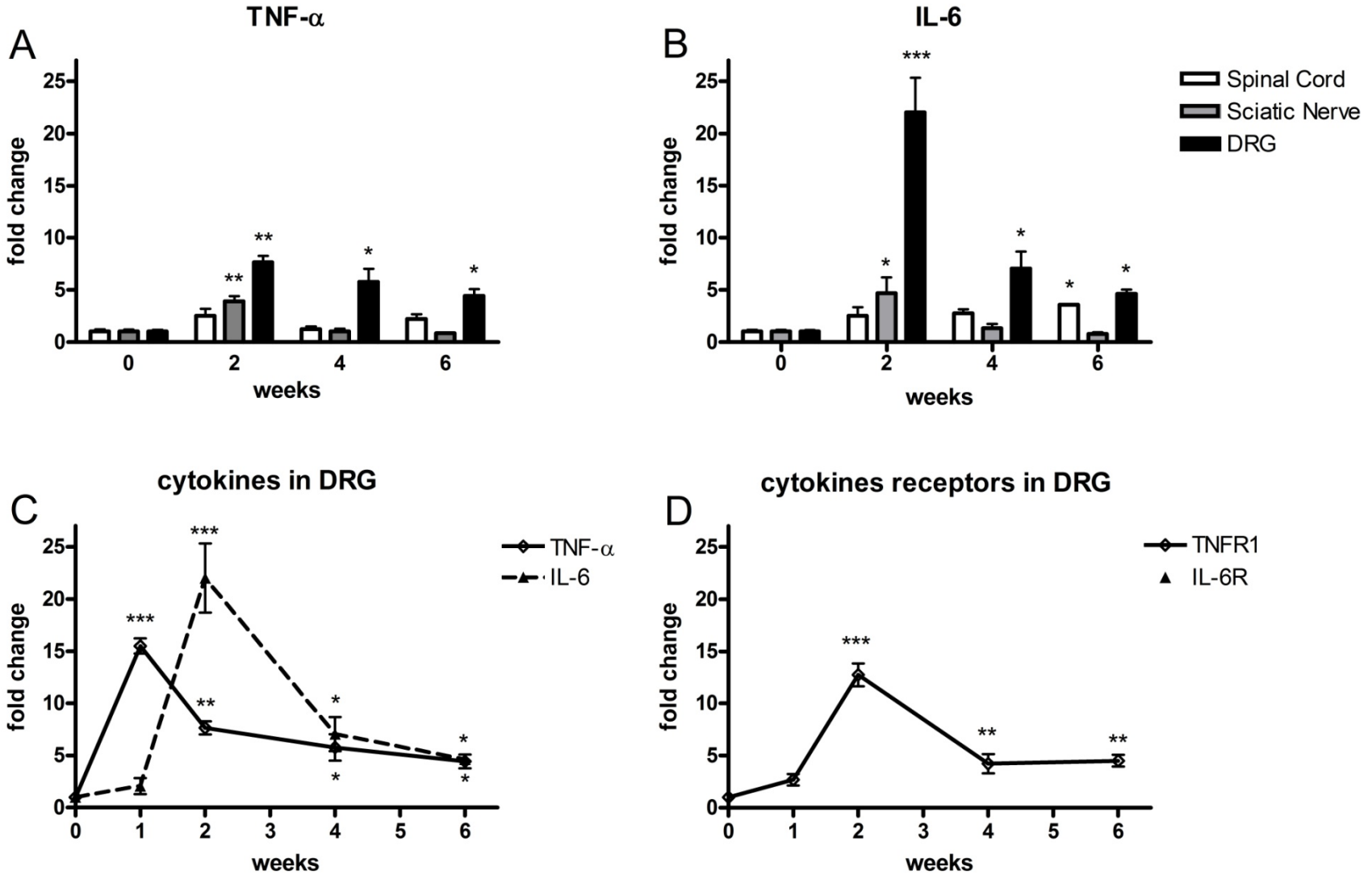

Fig. 1. Expression of TNF-α, IL-6 and their receptors on different nerve tissue during Bortezomib treatment. Levels of both cytokines were sustainably high until the end of treatment on DRG , whereas they were just slightly increased in sciatic nerve at 2 weeks and on spinal cord at the end. Only a significant increase of IL-6 at the 6 weeks was observed on spinal cord (A and B). Expression peak of TNF-α in DRG preceded IL-6 and TNFR1 peak (C and D). Values expressed as a mean and SEM . * P<0.05,**P<0.01,***P<0.001, vs basal group. *

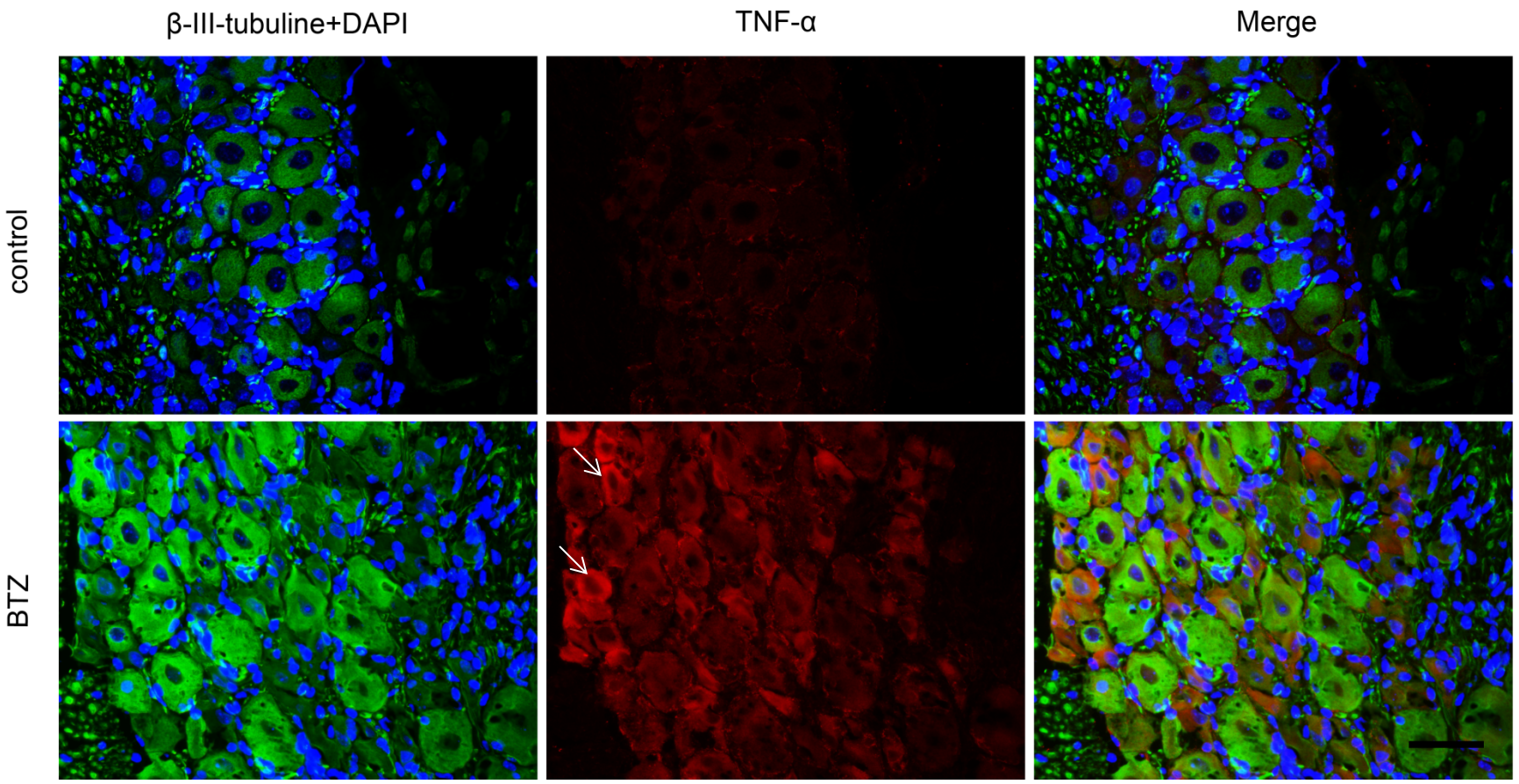

Fig. 2. Sections of DRGs immunolabeled against β-III-tubulin (green), DAPI (blue) and TNF-α (red), from a control (up) and an animals treated with BTZ for 1week (down). TNF-a collabels with β-III-tubulin, indicating that BTZ increases TNF-α expression on neurons specially on small ones (white arrows). Scale bar; 50 µm

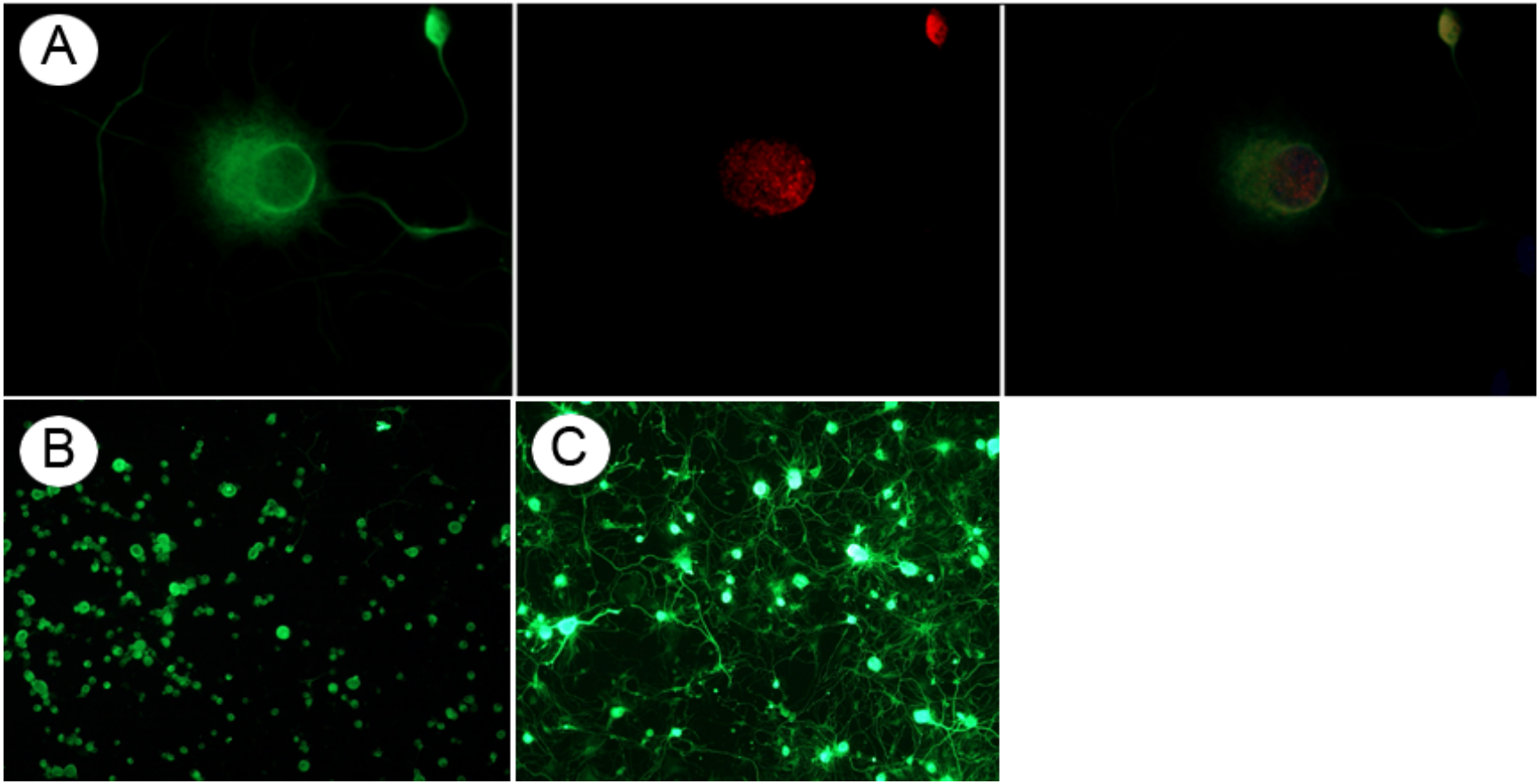

Fig. 3. Dissociated primary neurons from dorsal root ganglia of BTZ treated animals for 2 weeks, double-staining against B-III-tubuline (in green) and TNF-α (in red, A). TNF-a was mainly localized on neuronal cell body and was also present in neurites that suffered swelling, indicating pathological distribution of this cytokine along the neurite (A). Dissociated DRG neurons from control animals (B) and BTZ treated animals for two weeks (C), labeled with B-III-tubuline. Neurons from treated animals showed increased neurite elongation at 24h in culture compared to control ones. 50x magnifications A and 10x magnification in B -C

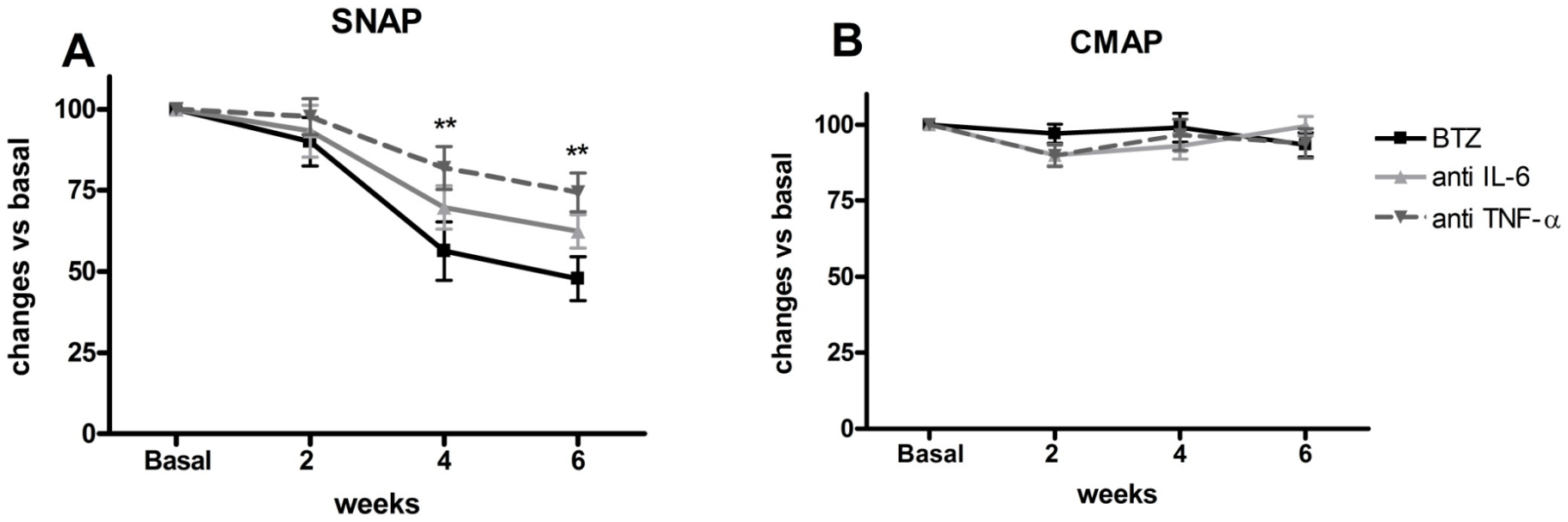

Fig. 4. Mean amplitude of the digital nerve SNAP (A) and the plantar muscle CMAP(B), stimulating at the sciatic notch. Values are expressed as percentages with respect to baseline. Both anti-TNF-α and IL-6 treatments partially maintains the decrease of the SNAPs , but only significantly on anti-TNF group. CMAP were not altered by any treatment. Error bars SEM. * $P<0.05$,**$P<0.01$.

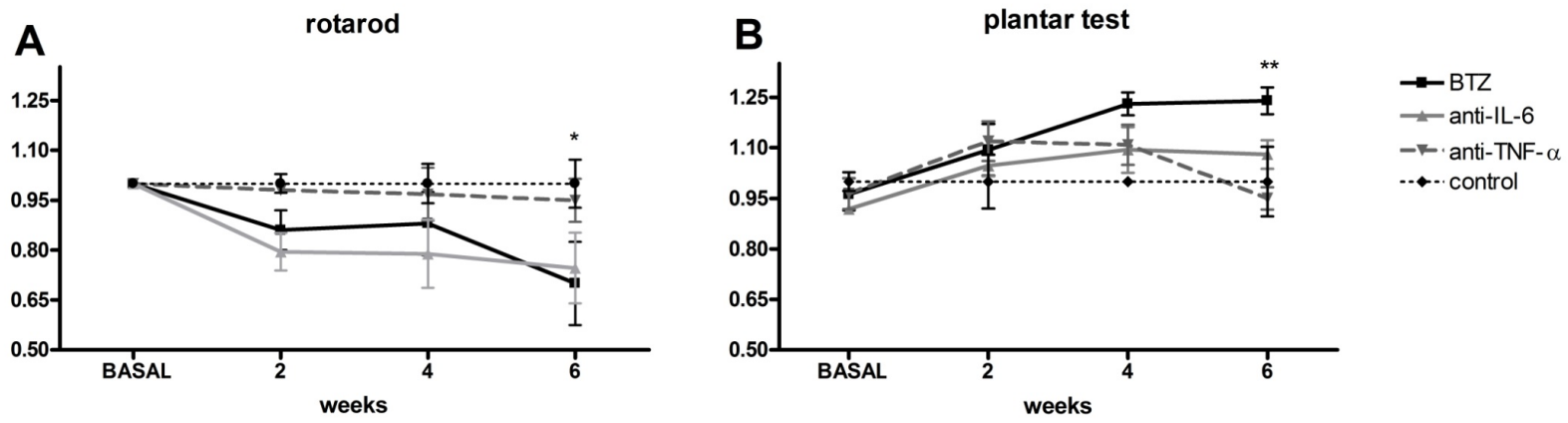

Fig. 5. Rotarod test results, expressed as time of maintenance in the rotating rod relative to baseline (A). Algesimetry test results expressed as time to withdrawal to hot pain stimulation. (B). All the groups were treated during 6 weeks. Anti-TNF -α treatment preserved the sensory-motor function and reverts the hypoalgesia, in contrast to BTZ and BTZ+anti IL-6 groups . Values are expressed as percentage with respect to baseline.

Error bars SEM. * $P<0.05$ ** $P<0.01$

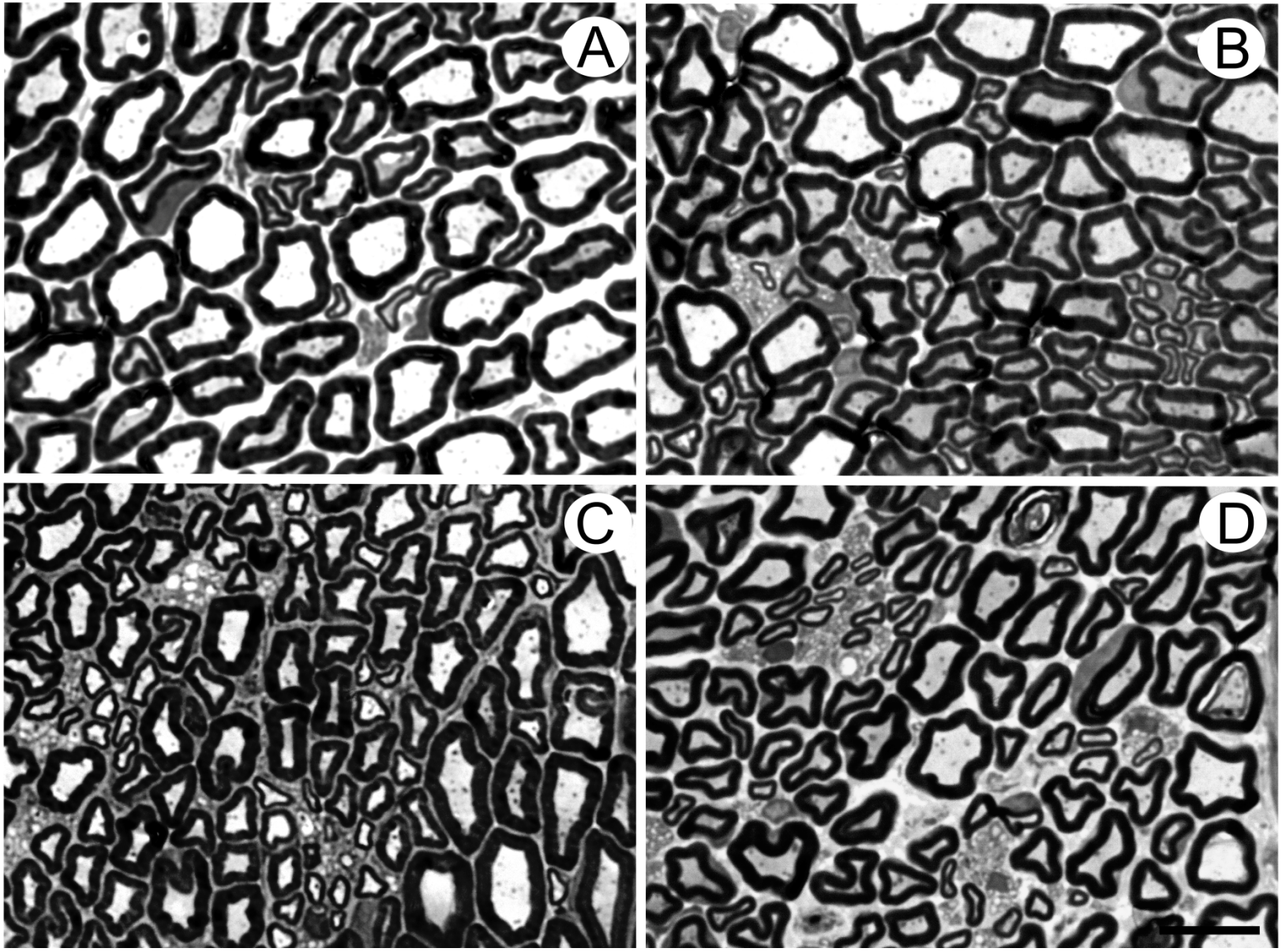

Fig. 6. Semithin sections of sciatic nerve at midthigh, in control animals (A), after 6 weeks of treatment with BTZ (D) or in co-treatment with anti TNF-α (B) or anti IL-6 (C). Decreased density of myelinated fibers by BTZ was prevented with anti TNF-α treatment.100x magnification. Scale bar; 20 µm

	nº of myelinated fibers	nº of unmyelinated profiles
CNTRL	4054 ± 157*	21 ± 2.05*
anti -TNF-α	3837 ± 292*	20 ± 3.71*
anti-IL-6	3792 ± 475	13 ± 5.10
BTZ	3548± 55	11 ± 5.82

Table 1. Estimated counts of myelinated nerve fibers of the sciatic nerve at midthigh and of unmyelinated intraepidermical fibers at the skin paw. Values expressed as mean and SD. *P<0.05 vs BTZ group

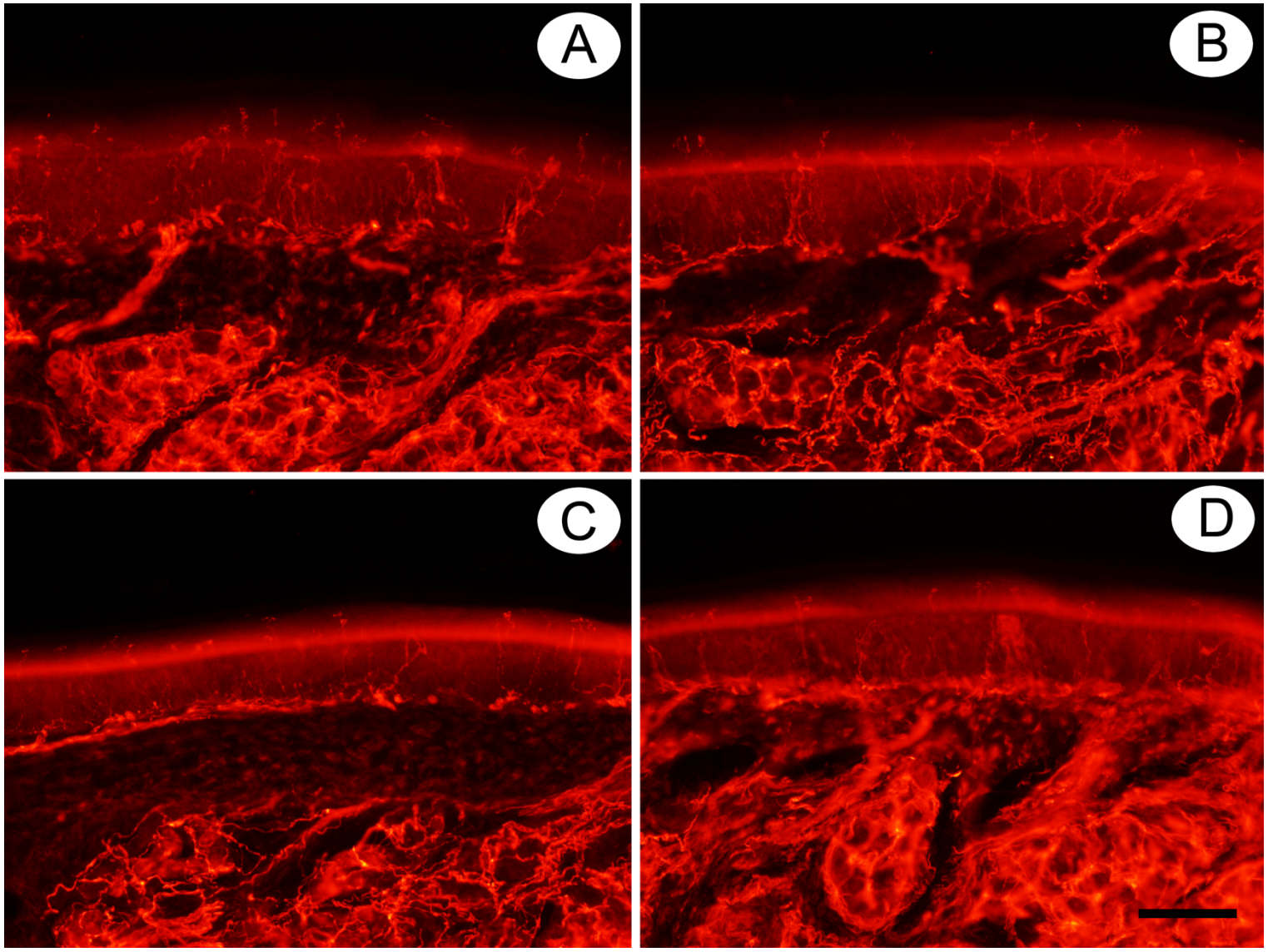

Fig. 7. Sections of skin pads immunolabeled against PGP 9.5. Images from a representative hind paws of a control (A), anti TNF-α (B) anti IL-6 (C) and BTZ (D) animals. Estimated counting of ummyelinated fibers (D). Number of intraepidermical profiles was significantly higher in anti TNF-α respect to BTZ treatment. 20x magnification Scale bar; 100 µm

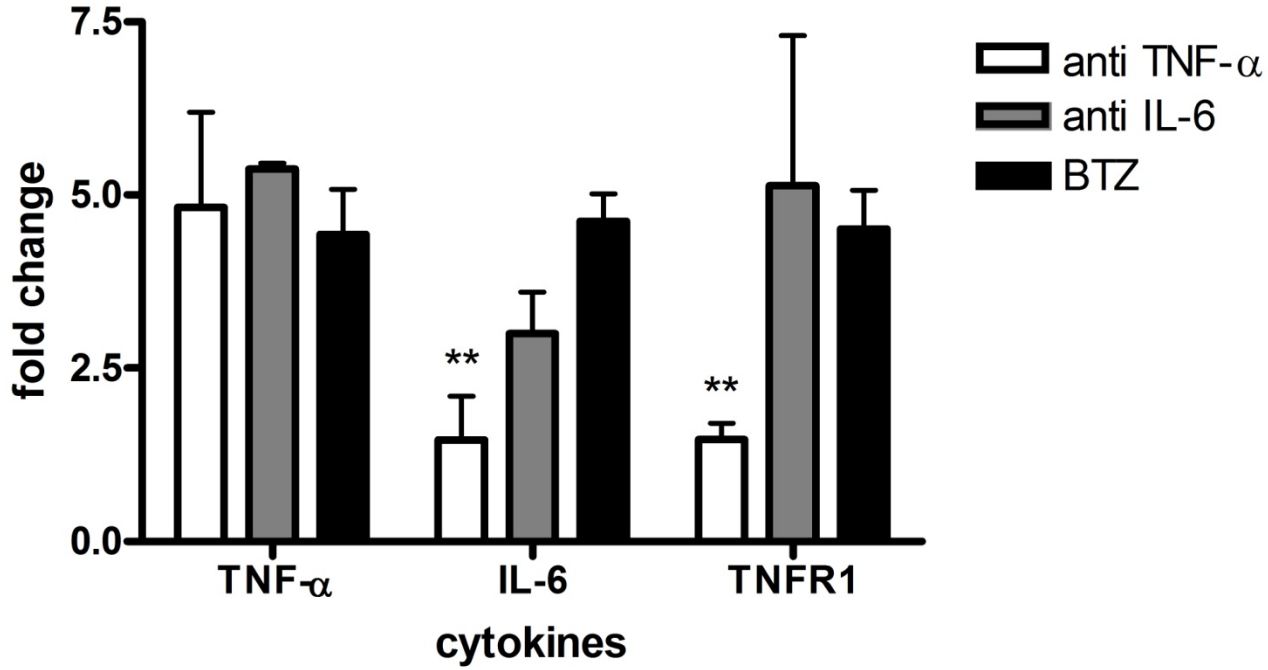

Fig. 8. Expression of TNF-α, IL-6 and their receptors on DRG at the end of the cotreatments. Anti -TNF-α cotreatment not affect up regulation of TNF-α but downregulate levels of TNFR1 and IL-6 expression , whereas no significant changes were observed IL-6 treatment. Values expressed as a mean and SEM . ** P<0.05 vs BTZ